

42

THE GENERALIZED VALENCE BOND VIEW OF MOLECULES; THE BH_n SERIES*

W.A. GODDARD III and R.J. BLINT

*Arthur Amos Noyes Laboratory of Chemical Physics**, California Institute of Technology,
Pasadena, California 91109, USA*

Received 11 April 1972

The low-lying states of B, BH, BH₂, and BH₃ are analyzed in terms of the orbitals obtained from generalized valence bond (GVB) calculations. We find that the geometries, symmetries, and qualitative form of the potential surfaces can be understood in terms of simple ideas involving the atomic orbitals. These same ideas can be used in many other systems.

1. Introduction

The Aufbau or building-up principle combined with the Mulliken and Hund orbital correlation diagrams [1] has been very successful in leading to useful predictions of the symmetries of excited states of molecules and when combined with the Walsh diagrams [2] has been quite useful in predicting qualitatively the geometries of polyatomic molecules. These important concepts were developed in terms of molecular orbitals and based on the Hartree–Fock (HF) method for wavefunctions. Despite these successes, there are some difficulties with these interpretations since the Hartree–Fock method leads to very poor wavefunctions as atoms are pulled apart (bond dissociation).

An alternative approach, the valence bond (VB) method, provides a proper description of bond dissociation but generally leads to poor quantitative results. We have modified the usual VB method by solving for the orbitals self-consistently as in the Hartree–Fock method [3, 4]. This leads to energies better than the Hartree–Fock values and in addition leads to a proper description of bond dissociation. This method { called the *generalized valence bond* (GVB) method [4] }

leads to an orbital description closely related to the usual VB description and hence allows convenient interpretation of the wavefunction.

We find that simple analyses of the GVB wavefunctions of atoms leads to an Aufbau-type principle that allows qualitative predictions of the symmetries and geometries of the excited states of molecules. However, this Aufbau principle does not involve the Mulliken–Hund or Walsh-type correlation diagrams. This principle, which was developed from the results of ab initio GVB calculations† on BH, will be illustrated here for the case of BH_n molecules.

2. Wavefunction

For a system with two bonds, a valence bond (VB) configuration has the form

$$\alpha[\phi_a \phi_b \phi_c \phi_d (\alpha\beta - \beta\alpha)(\alpha\beta - \beta\alpha)],$$

which we denote as

a	b
c	d

* Partially supported by a grant (GP-15423) from the National Science Foundation.

** Contribution No. 4433.

† These calculations used gaussian basis functions with a primitive (11s5p3d/6s3p) set contracted to (7s3p1d/3s1p).

(here a and b are singlet paired as are c and d). These orbitals can be bonded more than one way and the valence bond wavefunction may be taken as

$$C_1 \begin{bmatrix} a & b \\ c & d \end{bmatrix} + C_2 \begin{bmatrix} a & c \\ b & d \end{bmatrix}, \quad (1)$$

where the orbitals are generally taken as (hybridized) atomic orbitals. In the generalized valence bond (GVB) method [3, 4] we use wavefunctions of the form in (1) but allow every orbital (including nonbonding orbitals) to be singly-occupied (but non-orthogonal) and solve variationally for the optimum such orbitals (analogous to the procedure in HF). In addition, the coupling coefficients of (1) are optimized. (This procedure is used for various numbers of electrons and spins and has also been referred to as the SOGI method [3].) In diagrams of the type in (1),



indicates singlet pairing of the orbitals ϕ_a and ϕ_b , and



indicates triplet pairing of the orbitals.

2.1. The B atom

The usual Hartree–Fock (and valence bond) wavefunction for the ground state (2P) of B atom has the form

$$\alpha(\phi_{1s} \alpha \phi_{1s} \beta \phi_{2s} \alpha \phi_{2s} \beta \phi_{2pz} \alpha) \quad (2)$$

(where α is the antisymmetrizer or determinant operator). In the generalized valence bond (GVB) method we allow all orbitals to be different and replace the α by a suitable operator to retain the proper permutational (Pauli principle) and spin symmetry. The final wavefunction can be written in the VB-type form

$$\alpha[(\phi_{1s} \phi_{1s'} + \phi_{1s'} \phi_{1s})(\phi_{sx} \phi_{s\bar{x}} + \phi_{s\bar{x}} \phi_{sx}) \phi_{pz} \alpha \beta \alpha \beta \alpha] \quad (3)$$

$$= \alpha[\phi_{1s} \phi_{1s'} \phi_{sx} \phi_{s\bar{x}} \phi_{pz} (\alpha\beta - \beta\alpha)(\alpha\beta - \beta\alpha) \alpha],$$

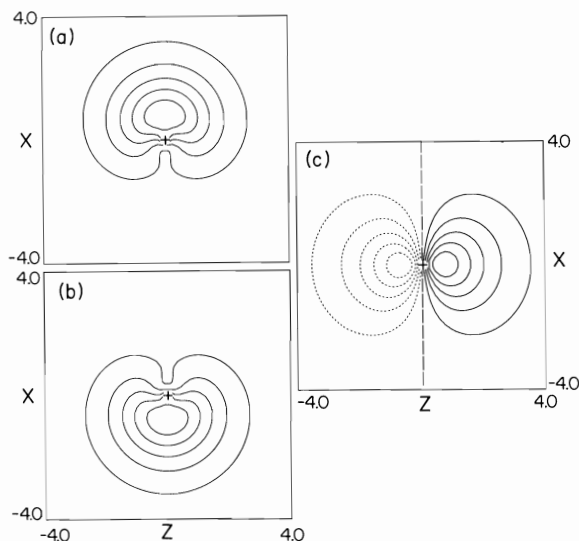


Fig. 1. The GVB valence orbitals of B atom (all quantities in atomic units). Long dashes indicate the nodal line; short dashes indicate negative amplitudes. The amplitude for the outer contour is 0.05 and the other contours are spaced at increments of 0.05. The + denotes the nucleus.

which we will denote as



The orbitals ϕ_{1s} and $\phi_{1s'}$ are referred to as core orbitals since they are similar to the usual 1s orbital (but radially split). These core orbitals are essentially unchanged upon bond formation and will be ignored in the following.

The p_z orbital (fig. 1c) is essentially the same as the HF $2p_z$ orbital, however the (2s) HF pair changes drastically upon going to GVB. These orbitals, sx and $s\bar{x}$, build in p character so as to attain the form

$$\phi_{sx} = C_1 \phi_{2s} + C_2 \phi_{2px}, \quad (5)$$

$$\phi_{s\bar{x}} = C_1 \phi_{2s} - C_2 \phi_{2px},$$

as shown in figs. 1a and 1b [5].

Combining the orbitals of (5) together, as in the many-electron wavefunction, leads to terms of the

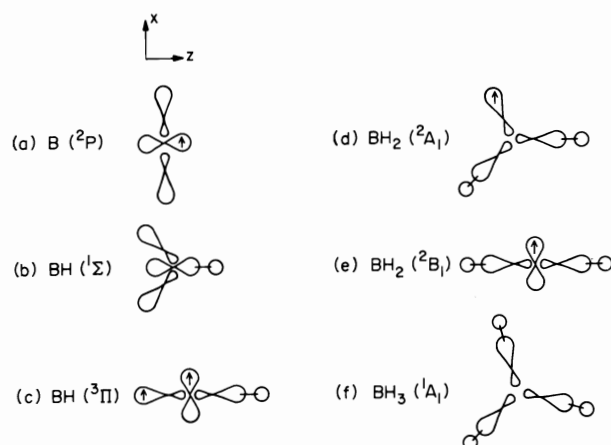


Fig. 2. Schematic representation of the orbitals of BH_n . A line connecting two orbitals indicates singlet pairing. An arrow indicates an unpaired orbital.

form*

$$\Psi_{(1,2)}^{GVB} = \phi_{sx} \phi_{s\bar{x}} + \phi_{s\bar{x}} \phi_{sx} \quad (6)$$

$$= C_1^2 \phi_{2s}(1) \phi_{2s}(2) - C_2^2 \phi_{2px}(1) \phi_{2px}(2).$$

Consequently, when both electrons 1 and 2 are on the same side of the atom (say in the $+x$ direction) the terms of (6) subtract, whereas they add when the electrons are on opposite sides of the atom. Thus the probability of the two electrons being on the same side is smaller than the probability of their being on opposite sides. This angular correlation [6] reduces the electron-electron repulsion energy (from that in HF) between these electrons and leads to a significant decrease in the energy [$0.015 h = 0.41 eV$ using (6) and $0.024 h = 0.65 eV$ using the full symmetry].

In discussions of the B atomic orbitals it is convenient to represent them schematically as in fig. 2a. Here the lobe orbitals sx and $s\bar{x}$ are shown pointing away from each other and perpendicular to the pz orbital.

* To retain the proper $2P$ symmetry of B, the second term of (6) must be replaced by

$$3^{-1/2} [\phi_{2px}(1) \phi_{2px}(2) + \phi_{2py}(1) \phi_{2py}(2) + \phi_{2pz}(1) \phi_{2pz}(2)].$$

However, the optimum orbitals using this form are essentially the same as those obtained using (5); hence no change occurs in the interpretation of the wavefunction.

2.2. BH molecule

Starting with the atomic orbitals of B and H we can form a 1Σ state†

sx	$s\bar{x}$
pz	Hx

(7)

or a 3Σ state

sx	$s\bar{x}$
pz	
Hx	

(8)

Since the pz and Hx orbitals have the same symmetry, the one-electron exchange terms should dominate the interaction energy, leading to a strongly bonding $1\Sigma^+$ state and a repulsive energy curve for the $3\Sigma^+$ state††.

In fig. 3 we show the orbitals for $1\Sigma^+$ as a function of internuclear distance, R . Here we see that the B pz orbital gradually delocalizes and hybridizes as the bond forms. As the bond is forming the nonbonding pair $[sx, s\bar{x}]$ rotates out of the way of the bond. This serves to reduce the overlap between the bonding and nonbonding pairs and hence to reduce the repulsive interactions between these pairs. The final angle between each lobe and the bond is 125° . These orbitals are indicated schematically as in fig. 2b.

Bringing the H in along the x axis leads from the atomic orbitals in (3) and (4) to

sx	$s\bar{x}$
pz	Hx

and

sx	$s\bar{x}$
pz	Hx

(9a, b)

† To have the proper rotational symmetry (Σ) the $[sx, s\bar{x}]$ pair function of (7) and (8) should have the form $\{C_1^2 \sigma(1) \sigma(2) - C_2^2 [\pi_x(1) \pi_x(2) + \pi_y(1) \pi_y(2)]\}$. However, inclusion of π_y terms led to little change in the shape of the orbital, and they were not included in the calculations reported here.

†† As mentioned above the splitting of the $(1s^2)$ core orbital has a negligible effect upon the bonding or interpretation of the wavefunctions. For this reason the core orbitals were kept doubly occupied in the calculations reported herein on BH. However, the orbitals shown in fig. 1 come from a wavefunction in which the $1s$ pair was allowed to split. As a result the sx and $s\bar{x}$ orbitals in fig. 1 are smooth in the core region whereas the corresponding orbitals of figs. 3 and 5 have an orthogonality node.

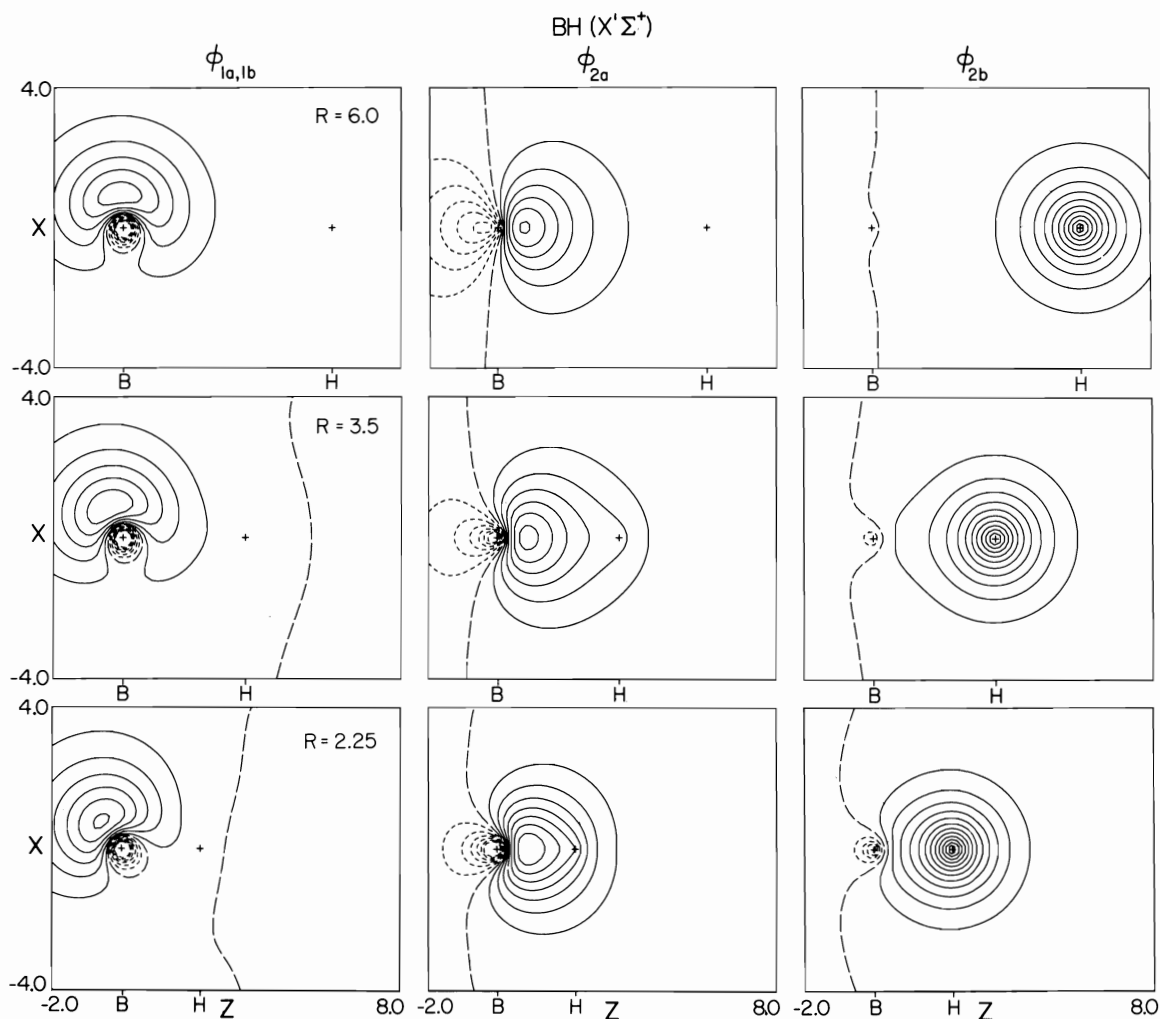


Fig. 3. The valence orbitals of the $^1\Sigma$ state of BH as a function of R . Only one (ϕ_{1a}) of the two nonbonding orbitals is shown; the other is symmetrically related. $R = 2.25 a_0$ is near R_e .

which describe the $^3\Pi$ and $^1\Pi$ states, respectively. At large R , these couplings lead to repulsive energy curves since the overlapping orbitals Hx and sx are not singlet-paired (the repulsive terms are approximately proportional to the square of the overlap between ϕ_{Hx} and ϕ_{sx} [7] and are quite analogous to the repulsions between different pairs of orbitals that are responsible for rotational barriers in molecules). However, for small R we can recouple the orbitals* of (9) as

$$\begin{array}{|c|c|} \hline sx & Hx \\ \hline pz & \\ \hline s\bar{x} & \\ \hline \end{array}
 \quad \text{and} \quad
 \begin{array}{|c|c|} \hline sx & Hx \\ \hline pz & s\bar{x} \\ \hline \end{array}
 \quad (10)$$

These couplings lead to attractive interactions between

* In the GVB calculations reported here, we optimized the spin coupling (SOGI [3]) which leads to admixtures of other couplings [as in (1)] noted in (9) and (10). However, the qualitative interpretation is not changed.

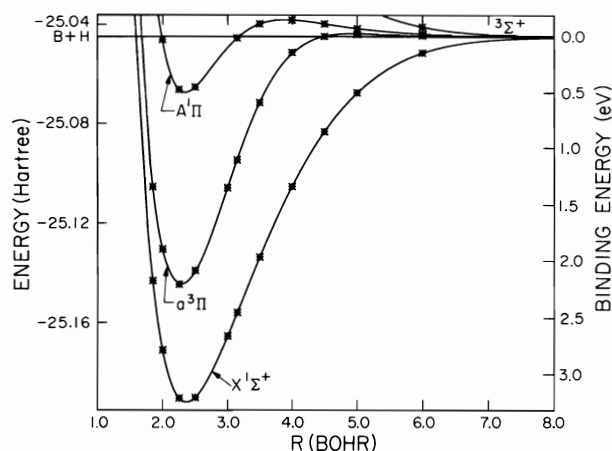


Fig. 4. The GVB energy curves for the low-lying states of BH.

ϕ_{sx} and Hx that are approximately proportional to the square of their overlap. However, (10) also leads to repulsive interactions (approximately proportional to the square of the overlap) between $\phi_{s\bar{x}}$ and Hx (and between $\phi_{s\bar{x}}$ and ϕ_{sx}). Thus (10) can lead to bonding only if sx and $s\bar{x}$ are sufficiently different so that $S_{sx,Hx}$ is large while $S_{s\bar{x},Hx}$ is small. However, as shown in fig. 1, the atomic angular correlation leads to just such splittings in ϕ_{sx} and $\phi_{s\bar{x}}$, and hence we may expect bonding in the $^3\Pi$ and $^1\Pi$ states of BH. Indeed, these states are bound as shown in fig. 4.

For large R the couplings in (10) cannot describe the ground state of B atom. Consequently, the recoupling and concomitant bonding do not occur until R decreases enough so that the bonding interactions of sx and Hx overcome the effect of promoting the state of the B atom.

The orbitals for the $^3\Pi$ state are shown as a function of R in fig. 5 (and indicated schematically in fig. 2c). Here we see continuous changes in the orbitals with R . Indeed, comparing the orbitals at $R = 2.25 a_0$ (near R_e) with those at $R = \infty$, we see that the GVB orbitals of the molecule are rather close in shape to the GVB atomic orbitals, which justifies the analysis above [e.g., (9) and (10)].

Examining fig. 5 closely we see that the singlet coupled pair (ϕ_{2a} and ϕ_{2b}) of the atom changes continuously into the bonding pair of the molecule while the nonbonding orbital on the H becomes the nonbonding orbital of the molecule. These changes are

quite comparable to those that occur in chemical reactions (see ref. [4]). Even the phase change expected (see refs. [4, 8]) in the nonbonding orbital (ϕ_{3a}) occurs. The potential humps in the Π states are quite analogous in origin to the activation energies of chemical reactions, and indeed the process $B + H \rightarrow BH$ corresponds to a highly exothermic addition reaction.

2.3. BH_2 and BH_3 molecules

Starting with the orbitals of the ground state of BH, fig. 2b, we must ask whether BH_2 should be stable and if so what geometry and symmetry should it have. Just as for the Π states of BH, we can form a strong bond by pairing the second H with one of the lobe orbitals of fig. 2b, leading to fig. 2d. Thus, we would expect BH_2 to be a 2A_1 state with a bond angle of about 125° . Some increase in this angle should occur due to overlapping of orbitals in different bonding pairs, and indeed the experimental bond angle [9] is 131° (theoretical calculations [10]* have led to 129°).

A second state of BH_2 is obtained by starting with BH ($^3\Pi$) and bonding the second H to the lobe orbital as indicated in fig. 2e. This leads to the 2B_1 state of BH_2 which is indeed linear [9].

Starting with the 2A_1 state of BH_2 we would expect BH_3 to be planar with D_{3h} symmetry (after allowing for slight readjustments of the orbitals due to the new bond-bond interactions). At this point there are no more valence orbitals for bonding further H's. (However, we do have an empty π orbital that can be involved in coordinate bonds.)

2.4. Energy humps

Because of the recoupling involved in proceeding from (9) to (10), we expected and found an energy hump at large R . This hump is 0.15 eV for $^1\Pi$ and 0.03 eV for $^3\Pi$ and occurs at $3.9 a_0$ and $4.9 a_0$, respectively. The difference in the humps for these states is due to the difference in the exchange interactions between the nonbonding σ and π orbitals. Averaging we obtain an exchangeless hump of about 0.09 eV at $4.4 a_0$.

In proceeding from $BH(^1\Sigma)$ to $BH_2(^2A_1)$ we have a similar recoupling. Thus for large R ($> 4.4 a_0$) we expect a repulsive energy curve regardless of orienta-

* Calculations by L.R. Kahn and R.J. Blint; see ref. [11].

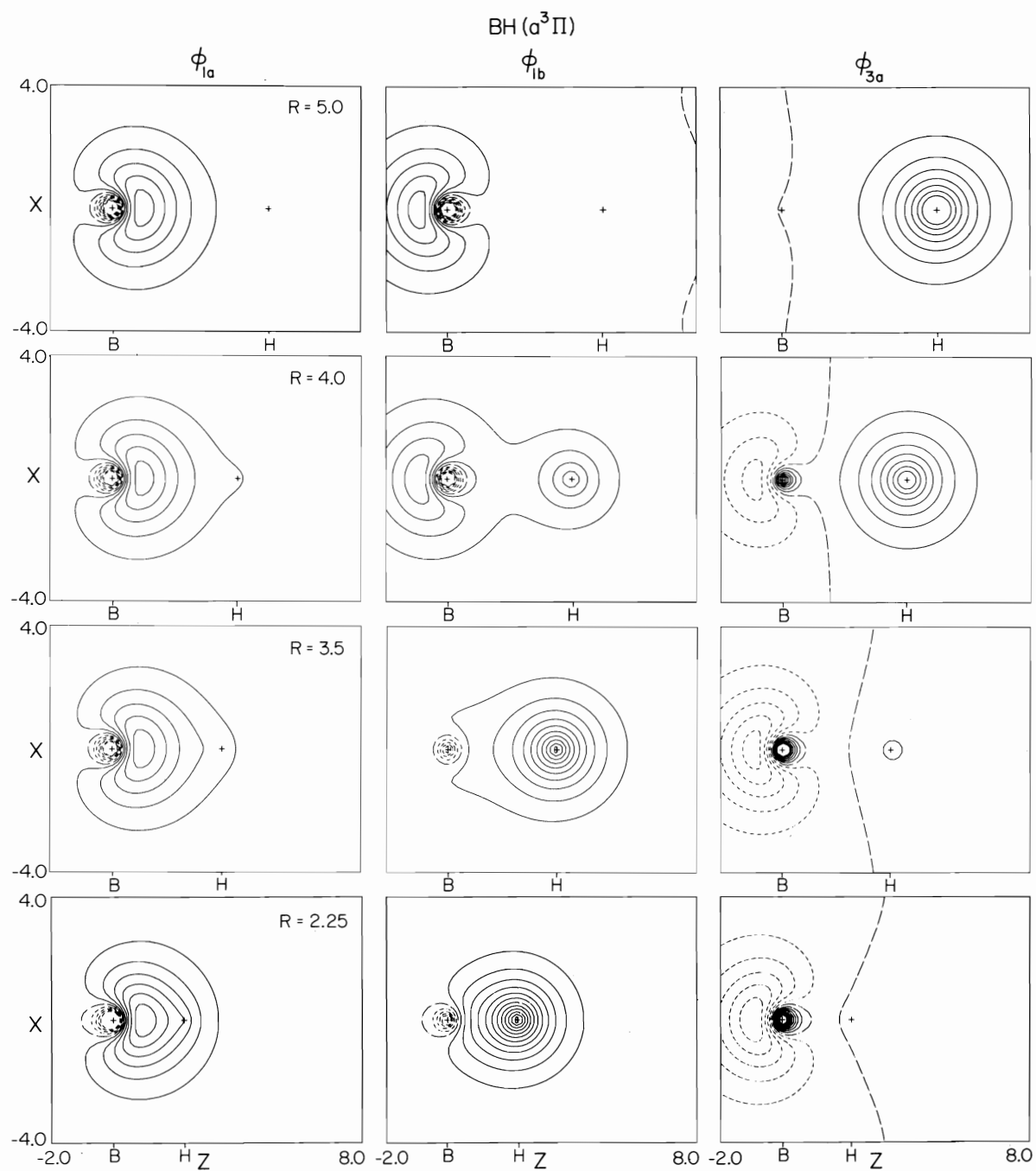


Fig. 5. The valence orbitals of the $^3\Pi$ state of BH as a function of R . The π orbital changes only very slightly with R and is not shown. The amplitudes are as in fig. 1. At large R , ϕ_{1a} and ϕ_{1b} are the B[s_x, s_x] pair; near R_e these orbitals are the bonding pair.

tion. However, for an angle of $\approx 125^\circ$ with respect to the bond axis and a second BH bond length of $\approx 4.4 a_0$, there should be a saddle point of about 0.03 to 0.09 eV in height. Inside this distance the energy should drop rapidly to that of BH_2 . On the other hand, for $\text{BH}(^3,^1\Pi) + \text{H} \rightarrow \text{BH}_2(^2\text{B}_1)$, and $\text{BH}_2(^2\text{A}_1) + \text{H} \rightarrow \text{BH}_3(^1\text{A}_1)$, we expect no humps along the minimum energy path.

From the form of the rotational breakoffs for $\text{A } ^1\Pi \leftrightarrow \text{X } ^1\Sigma$ in BH, it has long been presumed that the $\text{A } ^1\Pi$ state has a hump (at about $3.9 a_0$); however, the experiments do not yield the magnitude of the barrier [12]. No experimental results are available concerning humps in BH_2 and BH_3 .

3. Discussion and summary

From the GVB orbitals of B atom we can obtain qualitative predictions of the symmetries, geometries, and potential curves of the low lying states of BH_n . Thus, the trivalent nature of B is already apparent in the orbitals of the *ground* state (^2P) of B atom. There is no need to consider the presence of higher spectroscopic states to account for this trivalent character.

Similar analyses can be carried out for molecules formed from other atoms and lead to systematic predictions of the symmetries and geometries of large classes of polyatomic molecules. Thus valence-bond-type ideas can be used for predicting the sorts of things usually done with molecular orbitals in terms of Mulliken–Hund and Walsh-type correlation diagrams. In addition, the valence-bond ideas can be used

for discussing processes involving bond dissociation. For example, this approach leads to correct predictions of the occurrences of energy humps.

References

- [1] R.S. Mulliken, Phys. Rev. 32 (1928) 186, 761; Rev. Mod. Phys. 4 (1932) 1; F. Hund, Z. Physik 40 (1927) 742; 42 (1927) 93; 51 (1928) 759; 63 (1936) 719.
- [2] A.D. Walsh, J. Chem. Soc. (1953) 2260, 2266, 2288, 2296, 2301, 2306, 2321, 2325.
- [3] W.A. Goddard III, Phys. Rev. 157 (1967) 73; R.C. Ladner and W.A. Goddard III, J. Chem. Phys. 51 (1969) 1073.
- [4] W.A. Goddard III and R.C. Ladner, J. Am. Chem. Soc. 93 (1971) 6750.
- [5] R.J. Blint and W.A. Goddard III, J. Chem. Phys. 56 (1972), to be published.
- [6] J. Lennard-Jones and J.A. Pople, Phil. Mag. 43 (1952) 581.
- [7] C.W. Wilson Jr. and W.A. Goddard III, Chem. Phys. Letters 5 (1970) 45; C.W. Wilson Jr., Ph.D. thesis, California Institute of Technology (1970).
- [8] W.A. Goddard III, J. Am. Chem. Soc. 92 (1970) 7520; 94 (1972) 793.
- [9] G. Herzberg, Molecular spectra and molecular structure. III. Electronic spectra and electronic structure of polyatomic molecules (Van Nostrand, Princeton, 1967).
- [10] C.F. Bender and H.F. Schaefer III, J. Mol. Spectry. 37 (1971) 423.
- [11] L.R. Kahn and W.A. Goddard III, J. Chem. Phys. 56 (1972), to be published.
- [12] G. Herzberg and L.G. Mundie, J. Chem. Phys. 8 (1940) 263; J.W.C. Johns, F.A. Grimm and R.F. Porter, J. Mol. Spectry. 22 (1967) 435.